Atomic displacement and disorder in $LiNbO_3$ single crystal caused by high-energy ^3He ion irradiation: an x-ray absorption spectroscopy study

2009 J. Phys.: Condens. Matter 21 495401

(http://iopscience.iop.org/0953-8984/21/49/495401)

J. Phys.: Condens. Matter **21** (2009) 495401 (6pp) doi:10.1088/0953-8984/21/49/495401

Atomic displacement and disorder in $LiNbO_3$ single crystal caused by high-energy ^{3}He ion irradiation: an x-ray absorption spectroscopy study

T Vitova[1], M R Zamani-Meymian[2], K Peithmann[2], K Maier[2] and J Hormes[1]

[1] Institute of Physics, University of Bonn, Nußallee 12, 53115 Bonn, Germany
[2] Helmholtz Institute for Radiation and Nuclear Physics, University of Bonn, Nußallee 14-16, 53115 Bonn, Germany

E-mail: vitova@physik.uni-bonn.de and vitova@ine.fzk.de

Received 27 April 2009, in final form 21 October 2009
Published 12 November 2009
Online at stacks.iop.org/JPhysCM/21/495401

Abstract
Nb K-edge x-ray absorption fine structure spectra from a single lithium niobate (LN) crystal irradiated with high-energy ^{3}He ions of 41 MeV and from unexposed crystal as the reference material are compared. The differences in the x-ray absorption near edge structure (XANES) spectra are interpreted by simulating Nb K-edge XANES spectra with the FEFF8.2 code. It is found that displacements of Nb and Li atoms, as well as Li and O vacancies, are likely to cause structural disorder leading to change in the refractive index of LN and to diminished birefringence. This finding is in agreement with previous results obtained from SRIM-2003 simulations and transmission electron microscopy measurements.

1. Introduction

Lithium niobate (LN, $LiNbO_3$) is an important non-linear optical material widely applied in, e.g., holographic storage [1–4], waveguides, couplers [5], integrated modulators [6] and telecommunication networks. Waveguides are fabricated by in-diffusing or implanting LN crystals with metal ions, e.g. Ti [7, 8], or irradiating them with low-energy ions, e.g. O, F or He [9]. The surface of the crystal is used as a wall for the waveguide. The second wall is the thin layer of damaged material, where the ions are stopped (the Bragg peak). It has been observed that the refractive index (n) slightly changes in the region between the surface and the Bragg peak, when low-energy, low-mass ions pass through the material [10–12]. Peithmann *et al* strengthened this effect, by irradiating LN crystals with high-energy ^{3}He ions (41 MeV), and demonstrated how it can be used for fabrication of a novel type of polarization-selective embedded waveguide [13]. It was shown that the extraordinary refractive index (n_e) of LN is enhanced, whereas its ordinary refractive index (n_o) is reduced. The absolute values of n_e and n_o are nearly the same; hence the birefringence ($n_e - n_o$) of LN is diminished. The diminished birefringence was explained, using SRIM-2003 [14] simulations, by the loss of the axis of anisotropy, caused by Li, O and Nb lattice vacancies [15]. This effect is reversible, i.e. the refractive index change (Δn) is reduced at about 100 °C and disappears completely at about 500 °C. It is known that Li atoms diffuse in a LN crystal in the temperature interval 100–200 °C [16], whereas O and Nb atoms become mobile at higher temperatures [17]. It is assumed that with increasing temperature Li, Nb and O atoms diffuse to their initial positions in the crystal matrix, restoring the axis of anisotropy, i.e. the birefringence of the LN crystal [15]. These results are supported by TEM measurements [18]. Structurally disordered circular centres with about 4 nm diameter are visible in the TEM image of an irradiated LN crystal. The authors propose a model explaining them as the concentration of Li deficiencies.

X-ray absorption fine structure (XAFS) spectroscopy is a suitable tool for studying local structural changes around an element of interest in a compound. The x-ray absorption near edge structure (XANES) spectrum reflects changes in valency, site symmetry and significant structural damage. The

extended x-ray absorption fine structure (EXAFS) analysis provides information about the distance, number and type of near neighbouring atoms around an absorbing atom as well as the level of structural disorder in the material studied. However, revealing the structural changes causing Δn is a challenging task for XAFS spectroscopy. An exact probe of the irradiated spot with 1 mm^2 size is necessary. Moreover, significant damage must be present to be detected with the sensitivity of the method.

The goal of the XAFS study presented here is to probe the local environment of the Nb atoms in order to verify the structural damage indicated, i.e. Li, Nb and O lattice vacancies [15, 18]. For this purpose a single irradiated LN crystal with 40 μm thickness is studied. Nb K-edge XAFS spectra, measured within and outside of the irradiated spot, are compared. The XANES spectra are interpreted using simulations of Nb K-edge XANES spectra with the FEFF8.2 code [19].

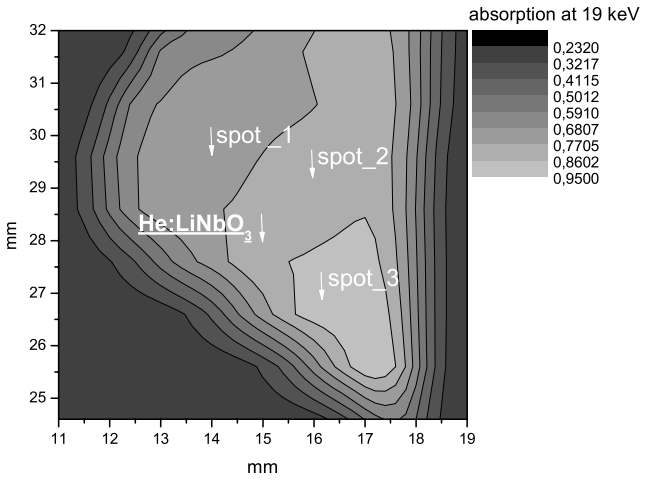

Figure 1. Absorption map of the irradiated single $LiNbO_3$ crystal with thickness 40 μm. The XAFS measurements are done at the irradiated spot, denoted with He:$LiNbO_3$, and at three spots, where the crystal is unexposed, denoted with spot_1, spot_2 and spot_3.

2. Preparation of the samples

A commercially available x-cut $LiNbO_3$ crystal was cut into $0.5 \times 10 \times 10$ mm^3 pieces, and polished and irradiated with ^{3}He ions with energy 41 MeV, at the Isochron cyclotron of the Helmholtz Institute for Radiation and Nuclear Physics, University of Bonn. The angle between the incoming ion beam and the crystal's surface was 90°. For more information about the irradiation process see [15]. The relaxation process of the activated Nb is as follows: (1) ^{93}Nb(^{3}He, ^{4}He)^{92}Nb; (2) ^{92}Nb captures an electron and transforms into ^{92}Zr with a half-life of 10 days; (3) ^{92}Zr relaxes by emitting a gamma ray with energy of 934 keV.

The thickness of one of the irradiated crystals was reduced to 40 μm after irradiation. The thinning was done with a grinding machine (Logitech PM5) using a glass grinding plate and Al_2O_3 powder suspension and this resulted in removing the Bragg peak from the crystal. We expect negligible influence on the interatomic distances, because after the thinning process no change in Δn is measured within the accuracy of the measurement.

3. Experiment, methods and data evaluation

The x-ray absorption spectroscopy (XAS) experiments were performed at the INE-Beamline at the ANKA 2.5 GeV synchrotron radiation facility at the FZK, Karlsruhe, Germany. For details about the instrumentation at this beamline, see [20]. For energy monochromatization, a Lemonnier-type [21] double-crystal monochromator equipped with a set of Ge(422) crystals was used. The x-ray beam size at the sample's position was about 500 μm $\times$ 500 μm.

The XAFS (XANES + EXAFS) spectra were recorded in transmission mode at room temperature using ionization chambers for measuring the incoming flux I_0 and the transmitted intensity I_1. Nb K-edge XANES spectra were measured in the energy interval from 18 930 to 19 140 eV with 1.7 or 0.6 eV step width and 1 s integration time. For energy calibration, a photon energy of 18 986 eV was set to the first inflection point of the K-edge spectrum of a niobium foil, measured simultaneously with the crystal. The data reduction of the Nb K-edge XANES spectra consisted of subtraction of a linear background fit to the pre-edge region from 18 936 to 18 970 eV and normalization of the spectra to an edge jump of one at 19 125 eV.

The ARTEMIS [22] program package was used for the EXAFS analysis. From the XAFS signals [$\chi(k)$] measured at the Nb K edge, a k range from 4.5 to 13 Å^{-1} was Fourier-transformed to R space using a k weighting of 1, 2 and 3 and a Hanning window with window sills dk equal to 2. The fit was performed in R space over a range from 1 to 5.5 Å. For the initial model the structure of $LiNbO_3$ (ICSD 28294) was used. The amplitude reduction factor (S_0^2) was fixed to 1 during the fit of the He:$LiNbO_3$ spectrum. This value was obtained by fixing the coordination numbers and varying S_0^2 during the fit of the non-irradiated $LiNbO_3$ FT-EXAFS spectrum. For all fits performed, the r-factor (overall goodness of fit) obtained was 0.02 or smaller, which means that the data and fit agree on average within 2% or better.

In the FEFF8.2 [19] calculations the EXCHANGE, SCF, FMS and XANES cards were used. The Hedin–Lundqvist self-energy was chosen as the exchange–correlation potential, which is the default setting of the EXCHANGE card. The calculations were done for a cluster of 200 atoms around Nb and no experimental broadening was added.

4. Results and discussion

4.1. XANES analysis

Figure 1 displays the absorption of the irradiated crystal with ≈40 μm thickness at 19 keV as a function of the x-ray beam position. The different areas represent spots from the sample with ±0.09 difference in absorption. The variations in absorption of the single LN crystal give us the opportunity to study the influence of thickness effects on Nb K-edge

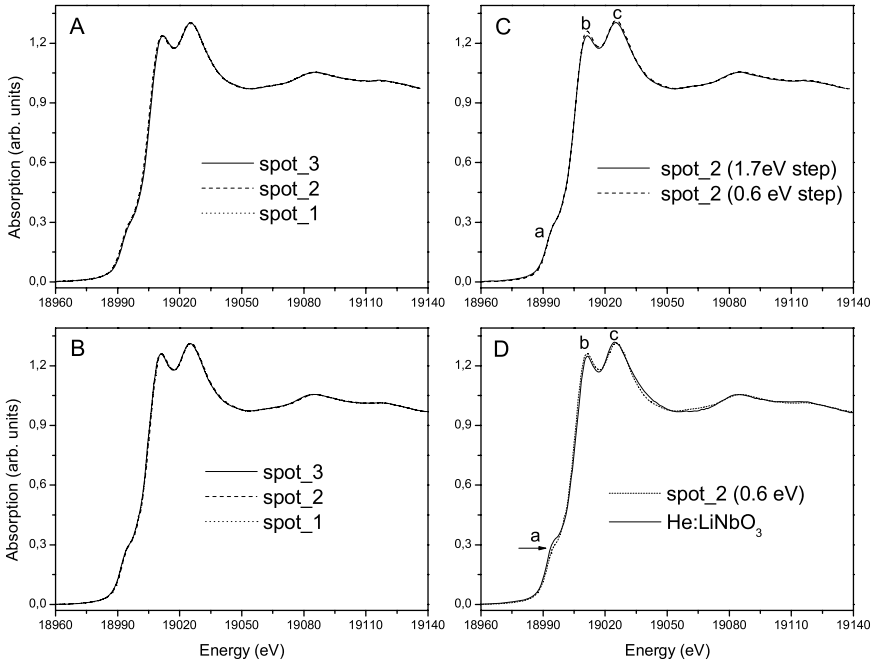

Figure 2. Nb K-edge XANES spectra of a single crystal of $LiNbO_3$ measured at different spots from the sample with 1.7 eV (A) or 0.6 eV (B) energy steps. Nb K-edge XANES spectra measured at spot_2 from the LN crystal with 1.7 or 0.6 eV energy steps (C). Nb K-edge XANES spectra measured in and outside of the irradiated spot (D) (see figure 1).

XANES spectra of LN. The spectra measured with 1.7 eV energy step width at positions from the sample marked with spot_1, spot_2 and spot_3 in figure 1 are plotted in figure 2(A). The three spectra are identical, which suggests that thickness differences of this order do not alter the XANES spectrum. These measurements were repeated with a 0.6 eV energy step width; the spectra are shown in figure 2(B). Nb K-edge XANES spectra, measured at spot_2 with 1.7 or 0.6 eV energy steps, are compared in figure 2(C). Obviously, the two spectra are identical in the pre-edge regions, denoted with a, whereas amplitude differences are visible in the WL regions, i.e. the b and c resonances of the spot_2 (0.6 eV) spectrum have higher intensity than the respective ones of the spot_2 (1.7 eV) spectrum. Nb K-edge XANES spectra measured at the irradiated and outside the irradiated spot with 0.6 eV energy step width are compared in figures 2(D) and 3. The differences in the WL regions of the two spectra are too small to be considered significant (see figure 3 peaks b and c). However, the increased intensity of the pre-edge shoulder of the $He:LiNbO_3$ spectrum is reproducible and significant and it certainly reflects structural changes occurring during the irradiation process (see figure 3(a)).

FEFF8.2 calculations based on two different models were carried out in order to explain the origin of the differences between the Nb K-edge XANES spectra measured within and outside the irradiated spot. The first model is motivated by study [23], which reports effect a (see figure 3), i.e. an increased intensity of the pre-edge resonance, and correlates it, in the case of octahedrally coordinated transition metal oxides, with displacement of the absorber atom from the centre of the octahedron. Figures 4 and 5 show some of the calculated spectra based on a systematic variation of atomic coordinates,

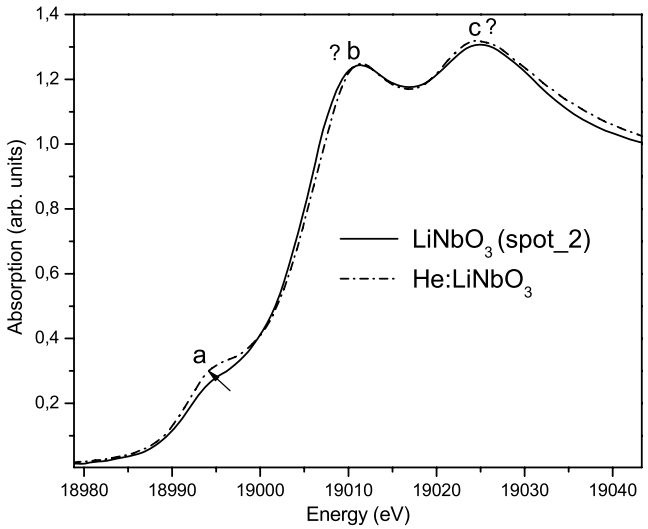

Figure 3. Nb K-edge XANES spectra measured in and outside of the irradiated spot (see figure 1).

i.e., the Nb atoms are shifted 0.01, 0.02 or 0.03 Å along the z axis, in negative (figure 4) or positive (figure 5) directions. The same calculations were performed by shifting the Nb atoms along the positive x and y and negative x and y axes. For most simulations, the amplitude of the pre-edge shoulder rises with the absolute size of the shift. This change in oscillatory strength is compensated by the features b and c in the WL region (see figure 5).

The second model implies the presence of Li and O vacancies in the structure. TEM studies in [18] suggest Li deficiency in the irradiated area. The vacancies are simulated

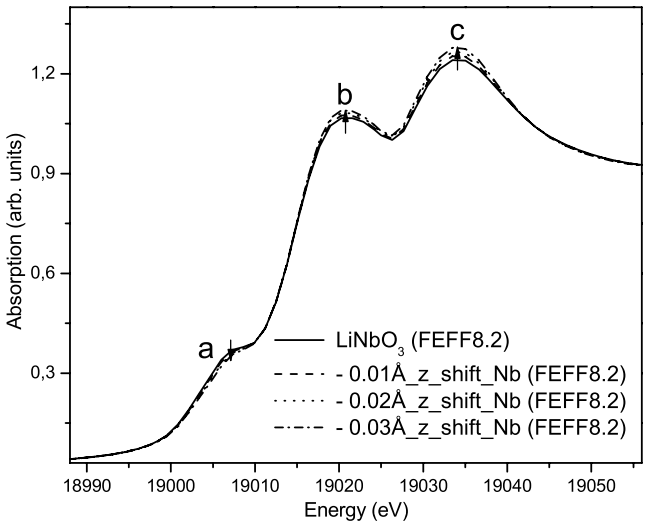

Figure 4. Nb K-edge XANES spectra of $LiNbO_3$ calculated with the FEFF8.2 code. A modified list of atomic coordinates is employed in most of the calculations, i.e., the Nb atoms are shifted 0.01, 0.02 or 0.03 Å along the z axis, in the negative direction.

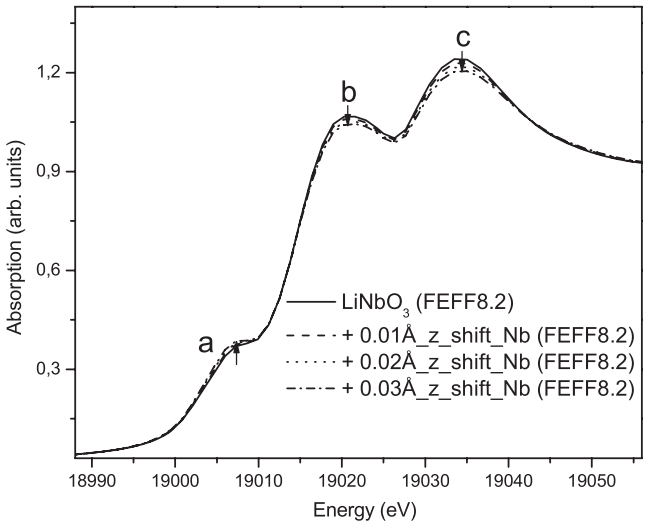

Figure 5. Nb K-edge XANES spectra of $LiNbO_3$ calculated with the FEFF8.2 code. A modified list of atomic coordinates is employed in most of the calculations, i.e. the Nb atoms are shifted 0.01, 0.02 or 0.03 Å along the z axis, in the positive direction.

by randomly removing of O and Li atoms/O atoms from the list of atomic coordinates. The Nb K-edge XANES spectrum converges after the averaging of about 15 calculated spectra. Figure 6 shows calculated spectra, with Li and O vacancies. Raised pre-edge resonance and redistributed intensities of the resonances in the WL region are visible. The amount of Li vacancies is exaggerated in the simulation, while the number of O vacancies is kept unchanged, in order to show their influence on the XANES' spectral shape. For charge compensation, 8% O vacancies are necessary for 45% missing Li atoms. The calculated spectra with simulated O vacancies are not shown here.

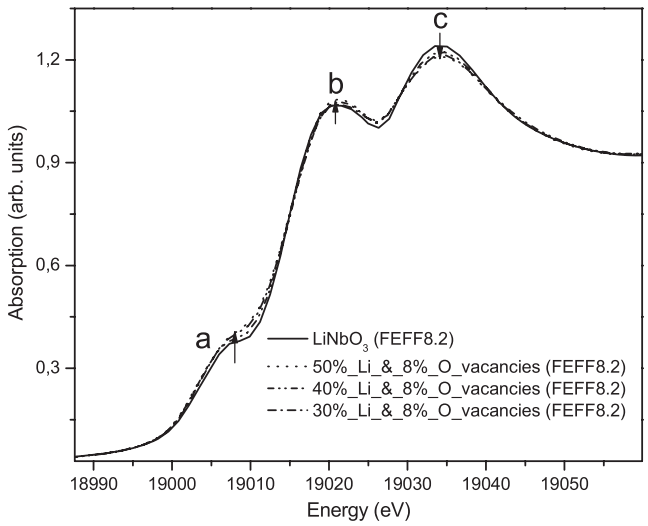

Figure 6. Nb K-edge XANES spectra of $LiNbO_3$ and $LiNbO_3$ with simulated Li and O vacancies calculated with the FEFF8.2 code.

The amplitude of the pre-edge shoulder decreases only in the case of the simulations shown in figure 4. This is an expected effect, as the Nb atoms move towards the centrosymmetric position in the oxygen octahedron. The pre-edge shoulder is rising in the remaining simulated XANES spectra. These findings indicate that XANES cannot be used alone to distinguish between these two models; hence they are both likely.

4.2. EXAFS analysis

Additional insights into the structural changes are provided by the EXAFS analysis. Figure 7 shows the EXAFS spectra in k (figures 7(A), (B)) and R (figures 7(C), (D)) space measured from the irradiated spot and at spot_2 of the sample. The first coordination shell of the He:$LiNbO_3$ spectrum was fitted with 5.0 ± 0.2 O atoms at 1.88 ± 0.01 Å and 3.5 ± 0.2 O atoms at 2.13 ± 0.01 Å. The structural parameters obtained from the spectrum measured at spot_2 are 3.6 ± 0.1 O atoms at 1.87 ± 0.01 Å and 3.0 ± 0.1 O atoms at 2.11 ± 0.01 Å. The fit values for the first coordination shell of the irradiated LN crystal tend to support the distorted octahedron model (see table 1). However, the structural parameters do not differ significantly, which excludes major local distortion and oxygen vacancy contributions. Nb vacancies do not dominate either, as the Nb coordination numbers change only slightly after irradiation. Changes are present in the vicinity of the second coordination shell, where differences in the Nb–Li distances are found (see table 1). This finding suggests that the applied irradiation has damaged the LN matrix by redistributing Li atoms. The Li coordination numbers remain the same within the error margins.

5. Conclusion

The simulations performed for the Nb K-edge XANES spectra indicate that displacement of Nb atoms as well as Li and O vacancies caused structural disorder. Within the sensitivity of

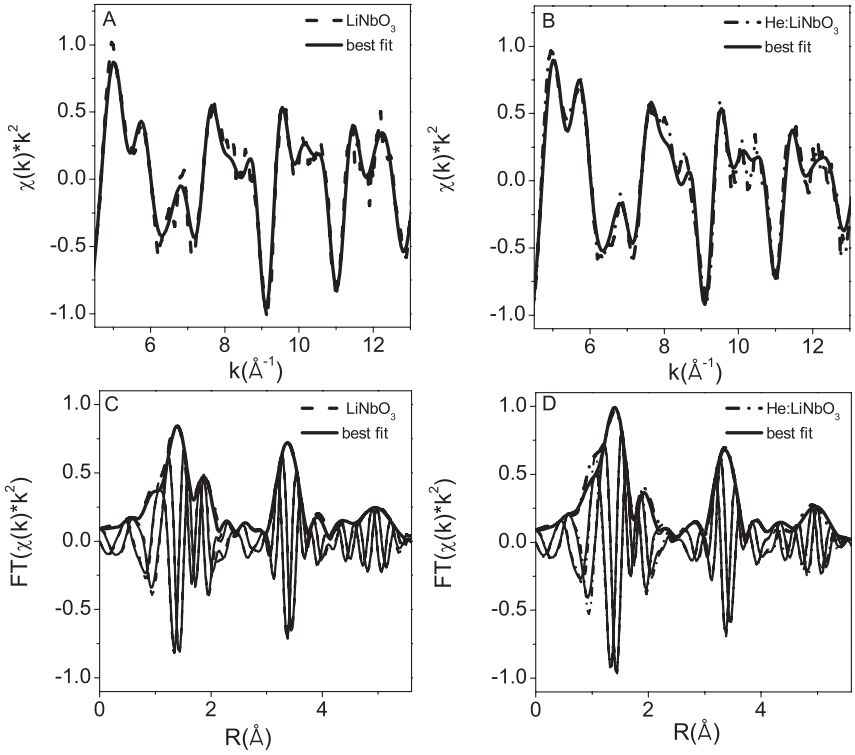

Figure 7. The $LiNbO_3$ (A), (C) and He:$LiNbO_3$ (B), (D) EXAFS spectra in k and R (magnitude, real and imaginary parts) space and their best fits.

Table 1. The results from the analyses of the $LiNbO_3$ and He:$LiNbO_3$ EXAFS spectra. The structural parameters are as follows: N: coordination number, R (Å): distance, σ^2 (Å^2): Debye–Waller factor and ΔE_0: energy shift of the ionization potential.

	$LiNbO_3$				He:$LiNbO_3$			
	R (Å)	N	σ^2 (Å^2)	ΔE_0	R (Å)	N	σ^2 (Å^2)	ΔE_0
Nb–O1	1.87 ± 0.01	3.6 ± 0.1	0.004 ± 0.001	2.3 ± 0.6	1.88 ± 0.01	5.0 ± 0.2	0.006 ± 0.001	3.3 ± 0.6
Nb–O2	2.11 ± 0.01	3.0 ± 0.1	0.004 ± 0.001	2.3 ± 0.6	2.13 ± 0.01	3.5 ± 0.2	0.006 ± 0.001	3.3 ± 0.6
Nb–Li1	3.04 ± 0.02	3.2 ± 1.0	0.004 ± 0.001	2.3 ± 0.6	3.10 ± 0.03	3.2 ± 1.5	0.006 ± 0.001	3.3 ± 0.6
Nb–Li2	3.24 ± 0.02	4.2 ± 1.3	0.004 ± 0.001	2.3 ± 0.6	3.16 ± 0.03	4.0 ± 1.6	0.006 ± 0.001	3.3 ± 0.6
Nb–Li3	3.47 ± 0.02	5.2 ± 2.5	0.004 ± 0.001	2.3 ± 0.6	3.45 ± 0.04	3.2 ± 3.0	0.006 ± 0.001	3.3 ± 0.6
Nb–Nb1	3.72 ± 0.01	4.3 ± 0.6	0.009 ± 0.001	-3.6 ± 1.0	3.71 ± 0.01	5.4 ± 1.0	0.007 ± 0.001	-8.3 ± 1.3
Nb–O3	3.80 ± 0.03	4.5 ± 1.5	0.004 ± 0.001	2.3 ± 0.6	3.84 ± 0.03	7.0 ± 1.3	0.006 ± 0.001	3.3 ± 0.6
Nb–O4	4.04 ± 0.03	3	0.004 ± 0.001	2.3 ± 0.6	4.08 ± 0.03	3	0.006 ± 0.001	3.3 ± 0.6
Nb–Nb2	5.06 ± 0.01	6	0.009 ± 0.001	-3.6 ± 1.0	5.02 ± 0.02	3.0 ± 1.1	0.007 ± 0.001	-8.3 ± 1.3
Nb–Nb3	5.42 ± 0.02	6	0.009 ± 0.001	-3.6 ± 1.0	5.40 ± 0.02	6	0.007 ± 0.001	-8.3 ± 1.3
Nb–O3–O2–Nb	4.93 ± 0.02	6	0.004 ± 0.001	2.3 ± 0.6	4.93 ± 0.01	6	0.006 ± 0.001	3.3 ± 0.6
Nb–O4–Nb1–Nb	5.70 ± 0.02	6	0.004 ± 0.001	-3.6 ± 1.0	5.67 ± 0.02	6	0.006 ± 0.001	-8.3 ± 1.3

the method, the FT-EXAFS spectra support the hypothesis of a redistribution of Li atoms. However, Li vacancies might be also present, this notion being supported by the large uncertainty in the Li coordination numbers.

The XAFS analyses support the result of disorder present in the geometrical structure of irradiated LN leading to loss of the axis of anisotropy [15, 18]. As a result, the refractive index is changed and the birefringence of LN is diminished [15]. More detailed information about the structural changes in a He:$LiNbO_3$ crystal could possibly be obtained by electron energy loss spectroscopy (EELS) at the Li and O K edges and x-ray diffraction topography.

Acknowledgments

The authors gratefully acknowledge financial support for project B1 within the DFG research unit 557, and the support by Boris Brendebach, Jörg Rothe and Kathy Dardenne at the INE-Beamline. We also thank the INE beamline team for critically reading the paper and giving valuable suggestions.

References

[1] Coufal H J, Psaltis D and Sincerbox G T 2000 *Holographic Data Storage* (Berlin: Springer)

[2] Shelby R M, Hoffnagle J A, Burr G W, Jefferson C M, Bernal M-P, Coufal H, Grygier R K, Guenther H, Macfarlane R M and Sincerbox G T 1997 *Opt. Lett.* **22** 1509
[3] Leyva V, Rakuljic G A and O'Conner B 1994 *Appl. Phys. Lett.* **65** 1079
[4] Breer S, Vogt H, Nee I and Buse K 1999 *Electron. Lett.* **34** 2419
[5] Alferness R C, Schmidt R V and Turner E H 1979 *Appl. Opt.* **18** 4012
[6] Ramaswamy V, Divino M D and Standley R D 1978 *Appl. Phys. Lett.* **32** 644
[7] Schmidt R V and Kaminow I P 1974 *Appl. Phys. Lett.* **25** 458
[8] Kip D 1998 *Appl. Phys.* B **67** 131
[9] Destefanis G L, Townsend P D and Galliard J P 1978 *Appl. Phys. Lett.* **32** 293
[10] Chandler P J and Townsend P D 1987 *Nucl. Instrum. Methods Phys. Res.* B **19/20** 921
[11] Glavas E, Zhang L, Chandler P J and Townsend P D 1988 *Nucl. Instrum. Methods Phys. Res.* B **32** 45
[12] Zhang L, Chandler P J and Townsend P D 1991 *Nucl. Instrum. Methods Phys. Res.* B **59/60** 1147
[13] Peithmann K, Zamani-Meymian M-R, Haaks M, Maier K, Andreas B, Buse K and Modrow H 2006 *Appl. Phys.* B **82** 419
[14] Ziegler J F, Biersack J P and Littmark U 1985 *The Stopping and Range of Ions in Solids* (Oxford: Pergamon)
[15] Peithmann K, Zamani-Meymian M-R, Haaks M, Maier K, Andreas B and Breunig I 2006 *Opt. Soc. Am.* B **23** 2107
[16] Nee I, Buse K, Havermeyer F, Rupp R A, Fally M and May R P 1999 *Phys. Rev.* B **60** R9896
[17] Birnie D P 1993 *J. Mater. Sci.* **28** 302
[18] Zamani-Meymian M R, Peithmann K, Maier K and Schmid H 2009 *J. Phys.: Condens. Matter* **21** 075402
[19] Ankudinov A, Ravel B, Rehr J J and Conradson S 1998 *Phys. Rev.* B **58** 7665
[20] Denecke M A, Rothe J, Dardenne K, Blank H and Hormes J 2005 *Phys. Scr.* T **115** 1001
[21] Lemonnier M, Coller O, Depautex C, Esteva J M and Raoux D 1978 *Nucl. Inst. Methods* **152** 109
[22] Ravel B and Newville M 2005 *J. Synchrotron Radiat.* **12** 537
[23] Shuvaeva V A, Yanagi K, Yagi K, Sakaue K and Terauchi H 1999 *J. Synchrotron Radiat.* **6** 367